14B.3 EVALUATING WATER VAPOR IN THE NCAR CAM3 CLIMATE MODEL WITH RRTMG/MCICA USING MODELED AND OBSERVED AIRS SPECTRAL RADIANCES

Michael J. Iacono *
Atmospheric and Environmental Research, Inc., Lexington, Massachusetts

1. INTRODUCTION

Representing the radiative impact of water vapor accurately, especially in the upper troposphere, is an essential component of effective global climate simulations. The direct comparison of modeled and observed spectral radiances provides a detailed means of assessing the simulation of radiative processes in a global climate model with satellite measurements. This work examines the simulation of water vapor in the National Center for Atmospheric Research (NCAR) climate model by comparing modeled and observed Atmospheric Infrared Sounder (AIRS) spectral radiances. A rapid and accurate spectral radiance algorithm developed at AER, the Optimal Spectral Sampling (OSS) model, has been fitted with the AIRS instrument function and is utilized to calculate clear sky radiances in the climate model for comparison to observed AIRS spectra. The RRTMG broadband longwave and shortwave radiation models developed at AER have also been implemented in CAM to examine the contribution of radiative transfer to the simulation of water vapor in the climate model.

2. MODELS AND SIMULATIONS

Due to its accessibility and wide application to climate studies the NCAR Community Atmosphere Model, CAM3.0 (Collins et al., 2006), is the climate model used for this analysis. CAM has been modified for this work to incorporate two additional components. RRTMG is a broadband, correlated k-distribution, longwave and shortwave radiative transfer model developed at AER for the Atmospheric Radiation Measurement (ARM) program (Clough et al., 2005) for application to general circulation models (GCMs). The accuracy of RRTMG is traceable to measurements through comparison to data-validated higher-resolution line-by-line models to ensure it retains a high level of accuracy (Iacono et al., 2008). RRTMG also utilizes the Monte-Carlo Independent Column Approximation, McICA (Barker et al., 2002; Pincus et al., 2003), which is an efficient, statistical method for representing sub-grid scale cloud variability including cloud overlap. RRTMG/McICA is being utilized in CAM3 for this project, though this analysis focuses on clear sky radiances. To model AIRS spectra in CAM, OSS is used to calculate radiance spectra for all 2378 channels of the NASA AIRS spectrometer with a computational speed that is roughly two orders of magnitude faster than a full spectrum radiance calculation with the line-by-line model LBLRTM. The primary spectral bands examined in this study include a large section of the region dominated by water vapor absorption (1340-1570 cm^{-1}), part of the spectrum sensitive to tropospheric temperature (700-750 cm^{-1}) and a small portion of the longwave window (937-952 cm^{-1}). Clear sky AIRS radiances are simulated with OSS for January and July 2004 using prescribed sea surface temperatures for two versions of CAM3. Simulations were performed both with the original climate model and with a modified version in which the radiation package was replaced with the RRTMG longwave and shortwave models. More information about the AER models is available at the AER radiative transfer web site (rtweb.aer.com).

3. AIRS MEASUREMENTS

Selected clear-sky modeled spectra from each simulation for various geographic regions are compared to observed, cloud-cleared AIRS version 4 L1B radiance spectra obtained from the NASA Goddard Earth Sciences Distributed Active Archive Center (DAAC) for the two months analyzed. All AIRS channels with bad or suspect quality control flags were excluded from the analysis. Also, AIRS data were only included for the two cross-track scan angles within 0.5 degree of nadir to correspond to the nadir calculations performed with OSS on the CAM-modeled profiles. Cloud clearing of the measured spectra was done by counting as clear those AIRS spectra that have a channel 857 (943.2 cm^{-1}) brightness temperature within 5 K of the AIRS L3 retrieved surface temperature over the tropical ocean regions examined.

* *Corresponding author address*: Michael J. Iacono, Atmospheric and Environmental Research, Inc., 131 Hartwell Avenue, Lexington, MA 02421-3105; E-mail: miacono@aer.com.

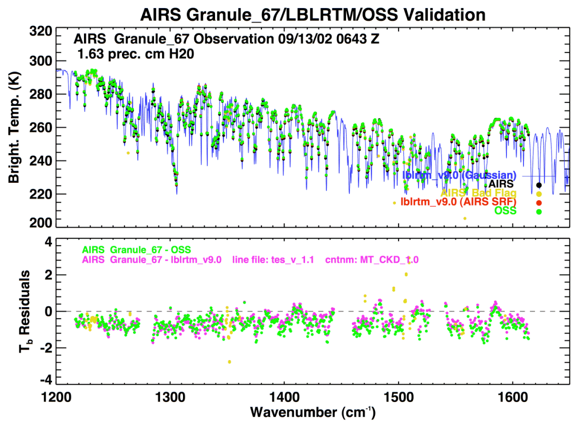

Figure 1. Spectral brightness temperatures (top panel) measured by AIRS at 0643 GMT on 13 September 2002 (black dots), modeled by LBLRTM and plotted at the AIRS resolution (red dots), and modeled by OSS and plotted at the AIRS resolution (green dots). The AIRS elements flagged as bad data (gold dots) and a Gaussian filtered line-by-line calculation (blue curve) are also shown. Spectral brightness temperature differences (bottom panel) between AIRS and LBLRTM (magenta dots) and between AIRS and OSS (green dots) are shown in units of K.

4. OSS VALIDATION

Before applying OSS to evaluation of the climate model, its accuracy was established with a three-way validation between AIRS, OSS, and the extensively validated line-by-line radiative transfer model, LBLRTM. A clear sky test case was chosen that corresponds to an AIRS observation over eastern Virginia from granule 67 at 0643 GMT on 13 September 2002. The input profile for the models was originally derived from a co-located atmospheric sounding. A retrieval was performed on the initial model-to-measurement radiance residual to reduce errors associated with the difference between the sounding temperature profile and that seen by the AIRS instrument. This modified input profile, including the retrieved temperature profile, was then used as input to the OSS and LBLRTM model calculations. The output from each model was then convolved with the AIRS instrument function to obtain calculated radiances at the spectral elements measured by AIRS and to facilitate a direct model to measurement comparison.

The result of this comparison over the 1200-1650 cm^{-1} spectral range in which water vapor is the dominant absorber is shown in Figure 1 in units of brightness temperature. The upper panel of Figure 1 shows the AIRS measurement (black dots), the AIRS elements that were flagged as bad data for this spectrum (gold dots), the LBLRTM calculation convolved with the AIRS instrument function (red dots), and the OSS calculation convolved with the AIRS instrument function (green dots). To provide spectral context, a LBLRTM line-by-line calculation of spectral brightness temperature that was smoothed with a Gaussian function to reduce the level of detail is also plotted (blue curve). Brightness temperature differences between AIRS and LBLRTM (magenta) and between AIRS and OSS (green) are plotted in the lower panel of Figure 1. Model to measurement brightness temperature residuals are generally less than 1 K across this band. In addition, model-to-model comparisons between OSS and LBLRTM for a large set of varying profiles show the two models to agree within 0.3 K or less across this spectral region. Overall, the OSS result is substantially similar to the result provided by the line-by-line approach, especially in the spectral regions of importance for water vapor absorption that are to be the focus of this research.

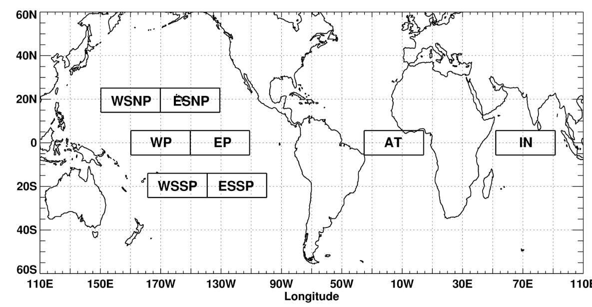

Figure 2. Pacific, Atlantic and Indian Ocean regions included in this analysis of modeled and observed cloud-cleared AIRS spectral radiances.

5. EVALUATING CAM TEMPERATURE AND WATER VAPOR

AIRS measured radiance data have been processed for January and July 2004 for comparison to CAM3 modeled spectra over several tropical ocean regions illustrated in Figure 2. Mean observed spectra are generated from all AIRS granules within each region. Since the models (CAM3_OSS and CAM3_RRTMG/McICA/OSS) calculate clear sky spectra at all grid points at six-hour intervals, these too must be processed for effective comparison to the measured radiances. If all modeled spectra were included in the analysis, the resulting mean spectra would be biased too moist since the presence of cloud generally increases the total water in the column from what would be present in a corresponding clear column. To account for this effect, the set of modeled radiances was reduced by excluding from the analysis all clear sky spectra for grid boxes in which a cloud cover of 0.3 or greater was present in any model layer above 700 mb. Clouds below this level are not considered, since most of the water vapor channels being examined (between 1340 and 1580 cm^{-1}) are opaque below this level for column water amounts that are generally present in the tropics. These values are found to provide a good compromise between ensuring the clearest spectra for the analysis while providing an adequate sample size.

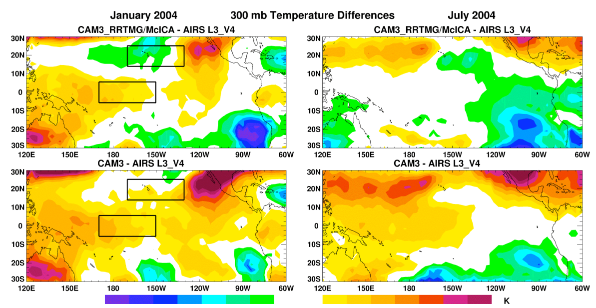

Figure 3. Temperature differences at 300 mb between two CAM3 simulations and the AIRS L3 retrieved values for January and July 2004. Black boxes indicate regions in which cloud-filtered brightness temperature spectra have been examined.

Although the objective of this work is to analyze modeled and observed spectral BT differences to evaluate the modeled temperature and water vapor, differences between the retrieved AIRS L3 (version 4) temperature and water vapor fields and those simulated by the CAM3 climate model have also been examined to place the spectral differences in context. Figure 3 shows differences in 300 mb temperature between the two CAM3 simulations and the AIRS L3 retrieved values over the Pacific Ocean during January and July 2004. The black boxes in Figure 3 represent two of the regions (WP and ESNP, see Figure 2) in which the brightness temperature spectra were examined. Both models are generally within about 1.5 K of the AIRS retrieved temperatures, though differences of up to 4 K or slightly larger are apparent in several regions. In the equatorial western Pacific region, both models are roughly 1 K warmer than the AIRS L3 temperature at this level.

Mean cloud-cleared AIRS L1B spectral brightness temperatures and differences between modeled and observed mean spectra over the 700-750 cm^{-1} spectral interval of relevance to the retrieval of tropospheric temperature are shown in Figure 4 for the western Pacific region during January 2004. Gaps in the plotted spectra indicate channels that were excluded due to their quality assurance settings as described above. Differences are shown between the CAM3/OSS simulation and the AIRS spectra (in blue) and between the CAM3_RRTMG/McICA/OSS simulation and the AIRS spectra (in red). Differences between each model result and the measurement show the CAM3 simulations to be similar and generally 1-2 K colder than the observation in these regions. This result is similar in sign as the result in Figure 3 for this region (models close to or cooler than the measurement), though the differences in Figure 4 are within the expected error (of 1-2 K) due to spatial and temporal sampling discrepancies between the model and observation. Figure 4 also indicates that in the eastern sub-tropical North Pacific, the differences are slightly larger in the upper troposphere (700-725 cm^{-1}) then in the middle to lower troposphere (725-750 cm^{-1}). Differences of this magnitude are consistent with those seen between CCM3-modeled and observed HIRS channel 4 radiances for winter seasons in the early 1980s (Iacono et al., 2003). This result (and similar results in the other regions) also suggests that brightness temperature differences in the water vapor channels that are of larger magnitude are primarily due to water discrepancies rather than temperature effects or deficiencies in the cloud filtering.

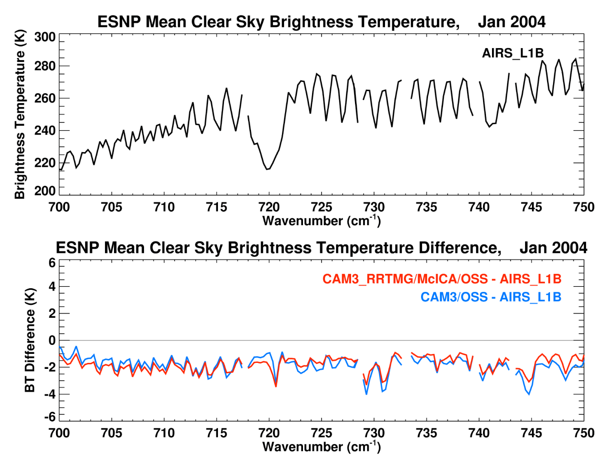

Figure 4. Mean cloud-cleared AIRS L1B brightness temperature spectra averaged over the western Pacific (ESNP) during January 2004 for the spectral interval of importance to tropospheric temperature (top panel), and the difference between two versions of CAM3 and AIRS measured spectra for this region (bottom panel).

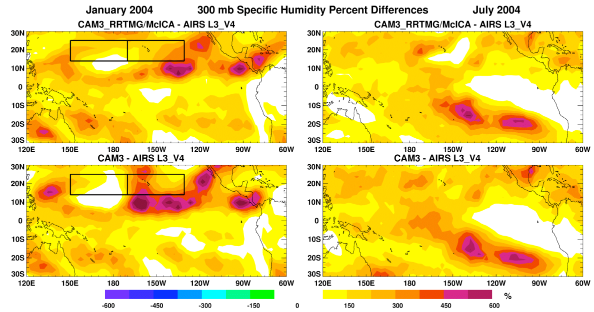

Figure 5. Water vapor specific humidity percent differences at 300 mb between two CAM3 simulations and the AIRS L3 retrieved values for January and July 2004. Black boxes indicate regions in which cloud-filtered brightness temperature spectra have been examined.

Water vapor differences between model and measurement are generally more significant than for temperature, though the magnitude is somewhat different depending on whether water vapor fields or spectral brightness temperatures are examined. Figure 5 shows percent differences in 300 mb water vapor specific humidity between the two CAM3 simulations and the AIRS L3 retrieved values over the Pacific Ocean during January and July 2004. The black boxes in Figure 5 represent two of the regions (WSNP and ESNP, see Figure 2) in which the brightness temperature spectra were examined. Both model simulations are generally significantly moister than the AIRS retrieved specific humidity at this level, especially just north of the equator in January and in the southern sub-tropics in July. Percent differences of up to several hundred percent are apparent in several regions. The model moist bias is somewhat larger in the ESNP region (indicated by rightmost black box in the left panels in Figure 5) than in the WSNP region.

Mean cloud-filtered AIRS L1B spectral brightness temperatures and differences between modeled and observed mean spectra over the 1340-1580 cm^{-1} interval dominated by water vapor absorption and emission are shown for the western subtropical North Pacific (WSNP) during January 2004 in Figure 6. As in Figure 4, differences are also shown between each model result and the measured spectra. Radiances in this spectral region are largely emitted from the middle to upper troposphere. Suspect channels are more frequent in this interval and are the cause of most of the numerous gaps, especially at higher wavenumbers. Across this spectral region, brightness temperature differences are generally 2-3 K and considerable spectral variation is apparent. The sign of the differences indicates colder brightness temperatures (and therefore moister conditions) in the model simulations, though some of the spectral difference may be due to temperature discrepancies. Calculations with a line-by-line model show that an increase in the total water column of about 15% in the tropics is needed to produce a decrease of about 1 K in top of the atmosphere BT in this spectral region (Iacono and Clough, 1996). This guide suggests that the brightness temperature differences in Figure 6 correspond to a modeled moisture bias

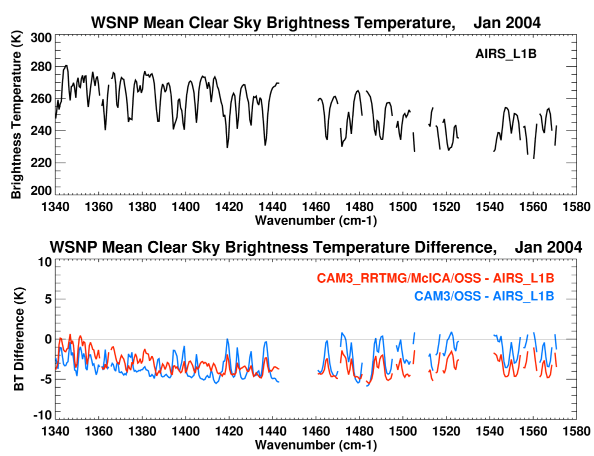

Figure 6. Mean cloud-filtered AIRS L1B brightness temperature spectra averaged over the western subtropical North Pacific (WSNP) during January 2004 for the spectral interval dominated by tropospheric water vapor (top panel), and the difference between two versions of CAM3 and AIRS measured spectra for this region (bottom panel).

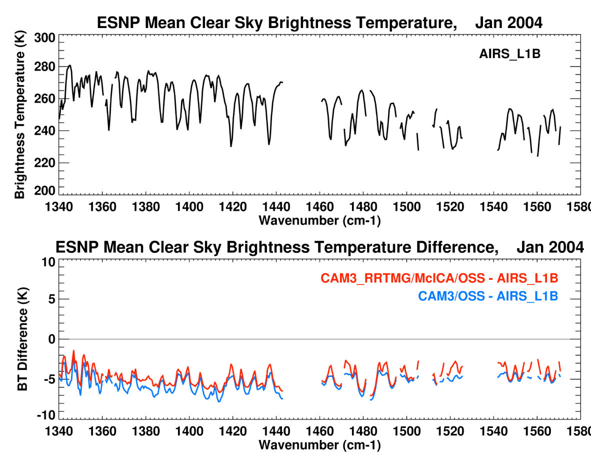

Figure 7. Mean cloud-filtered AIRS L1B brightness temperature spectra averaged over the eastern subtropical North Pacific (ESNP) during January 2004 for the spectral interval dominated by tropospheric water vapor (top panel), and the difference between two versions of CAM3 and AIRS measured spectra for this region (bottom panel).

on the order of 25-50% in the column and possibly more in individual layers, which is consistent with the 75-150% modeled moist bias at 300 mb in this region illustrated in Figure 5 through comparison of the specific humidity directly. Finally, some sensitivity in the choice of radiation model (the only difference between the simulations) is apparent in the spectral brightness temperature differences in Figure 6.

Mean cloud-filtered AIRS L1B spectral brightness temperatures and differences between modeled and observed mean spectra over the 1340-1580 cm^{-1} interval dominated by water vapor absorption and emission are shown in Figure 7 for the eastern subtropical North Pacific (ESNP) during January 2004. In this region, the model to observed spectral brightness temperature differences are considerably larger than those seen in the adjacent WSNP region (Figure 6) and average about 4-5 K across the band. This corresponds to a modeled moist bias of roughly 60-80% in the entire column in this region, with larger or smaller percent differences possible in specific vertical regimes. This is consistent with the higher percentage differences seen in the 300 mb specific humidity in Figure 5, which are roughly 200-250% in this region. Some sensitivity to the radiation model used in the simulation is again apparent, though this effect is generally small relative to the BT differences, and it is expected that any deficiencies in radiative transfer are not a significant contribution to the water vapor biases seen in this climate model.

6. CONCLUSIONS

The OSS algorithm has been used within CAM to model spectral radiances and thereby provide the capability to examine temperature and water vapor deficiencies in the climate model at high spectral resolution. This also provides an alternative closure method for evaluating the climate model with radiative transfer calculations and directly observed spectral radiances rather than comparing model fields with parameters retrieved from spectral radiances. Applying the data-validated radiation model, RRTMG, provides a means of establishing whether water vapor deficiencies are related to radiative transfer.

Within the spectral region of relevance to middle and upper tropospheric temperature (700-750 cm^{-1}), differences between modeled and observed brightness temperatures are generally less than 2 K and are mostly insensitive to the radiative transfer method. However, within the spectral region dominated by water vapor absorption (1340-1580 cm^{-1}), differences in brightness temperature of up to 5-10 K are present that vary spectrally and by geographic region. Differences in brightness temperature of this magnitude represent significant discrepancies in upper tropospheric water vapor amount of 50% or more in some tropical ocean regions in CAM3. While the brightness temperature differences in the water vapor spectral band are somewhat sensitive to the improved radiative transfer in some geographic regions, it is apparent that the treatment of radiation is not the primary cause of the simulated water vapor discrepancies.

7. ACKNOWLEDGMENTS

Funding for this project was provided by NASA under grant number EOS/03-0544-0471, and AIRS data were obtained from the NASA GES Distributed Active Archive Center.

8. REFERENCES

Barker, H. W., R. Pincus, and J.-J Morcrette, 2002: The Monte Carlo Independent Column Approximation: Application within Large-Scale Models. In Proceedings of the *GCSS-ARM Workshop on the Representation of Cloud Systems in Large-Scale Models*, May 2002, Kananaskis, AB, Canada.

Clough, S.A., M.W. Shephard, E.J. Mlawer, J.S. Delamere, M.J. Iacono, K. Cady-Pereira, S. Boukabara, P.D. Brown, 2005: Atmospheric radiative transfer modeling: a summary of the AER codes, *J. Quant. Spectrosc. Radiat. Transfer*, **91**, 233-244.

Collins, W.D., P.J. Rasch, B.A. Boville, J.J. Hack, J.R. McCaa, D.L. Williamson, B.P. Briegleb, C.M. Bitz, S.-J. Lin, and M. Zhang, 2006: The formulation and atmospheric simulation of the Community Atmosphere Model Version 3 (CAM3), *J. Climate*, **19**, 2144-2161.

Iacono, M.J., J.S. Delamere, E.J. Mlawer, M.W. Shephard, and S.A. Clough, 2008: Radiative forcing by long-lived greenhouse gases: Calculations with the AER radiative transfer models, submitted to *Geophys. Res. Letters*.

Iacono, M.J., J.S. Delamere, E.J. Mlawer, S.A. Clough, 2003: Evaluation of upper tropospheric water vapor in the NCAR community climate model (CCM3) using modeled and observed HIRS radiances, *J. Geophys. Res.*, **108(D2)**, 4037, doi:10.1029/2002JD002539.

Iacono, M.J., and S.A. Clough, 1996: Application of infrared interferometer spectrometer clear sky spectral radiance to investigations of climate variability, *J. Geophys. Res.*, **101**, 29439-29460.

Pincus, R., H. W. Barker, J.-J. Morcrette, 2003: A fast, flexible, approximate technique for computing radiative transfer in inhomogeneous cloud fields, *J. Geophys. Res.,* **108**, D13.